Brillouin Scattering Study of Acoustic Attenuation in Fused Quartz*

ALAN S. PINE
Lincoln Laboratory, Massachusetts Institute of Technology, Lexington, Massachusetts 02173
(Received 3 February 1969; revised manuscript received 5 May 1969)

The velocity and attenuation of 27–28-GHz longitudinal hypersonic waves in fused quartz have been measured for temperatures between 80 and 600°K. The data are obtained using high-resolution signal-averaging techniques of thermal Brillouin spectroscopy. The velocity, or Brillouin shift, is found to increase with temperature at a rate of ~0.011%/°K throughout the range. The attenuation, or linewidth, goes through a pronounced peak at a temperature of ~130°K. This sort of behavior usually indicates a structural relaxation mechanism for the hypersonic damping, as has been suggested for previous ultrasonic measurements in fused quartz. However, it is demonstrated that an anharmonic model involving three-phonon interactions can explain the absorption data with fewer adjustable parameters, which have better physical justification.

I. INTRODUCTION

THE velocity and attenuation of thermally excited longitudinal hypersonic waves in fused quartz have been measured for temperatures between 80 and 600°K. Phonon frequencies of about 27 GHz are probed by backward scattering of 6328 Å single-frequency laser light. High-resolution, multiscanned interferometry is employed to obtain adequate precision and signal-to-noise ratio.

The temperature variations of the damping and velocity of hypersound in fused quartz are similar to those measured by lower-frequency ultrasonic methods.[1] There is a prominent low-temperature peak in the absorption; the temperature at the peak increases slowly with frequency; and the maximum absorption increases slightly faster than the frequency. The velocity of hypersound increases with temperature. These results are in marked contrast to those obtained earlier in crystalline quartz at comparable frequencies.[2] In α-quartz, the damping increases monotonically with increasing temperature and the elastic constants generally soften. This discrepancy has led to the view that the excess absorption in the vitreous material is caused by a resonant interaction with thermally activated structural transitions. However, in this paper we demonstrate that the absorption data for fused quartz, particularly at hypersonic frequencies, are better explained by a simple anharmonic mechanism involving scattering of thermal phonons. The principal difference between silica and α-quartz arises from the branches of thermal phonons dominant in the interaction.

For fused quartz, there have been no microwave frequency studies of induced sound-wave propagation like those in α-quartz, because of the relatively high attenuation. Jones, Klemens, and Rayne[3] achieved the highest frequencies (~1 GHz) to date by conventional pulse-echo methods. Thermal Brillouin scattering, on the other hand, is admirably suited to probe this regime, since it is not restricted to low absorption. Several workers have recorded clear Brillouin spectra from fused quartz. Krishnan[4] and Flubacher *et al.*,[5] using mercury arc lamps and prism or grating spectrographs, were able to show that the hypersound was underdamped and its velocity close to the ultrasonic value. Thus, contentions that high-frequency sound could not propagate in "viscous" glasses could be dismissed.[6] Shapiro, Gammon, and Cummins[7] obtained more accurate results using a He-Ne laser and a Fabry-Perot interferometer. The first room-temperature spectra to resolve the natural linewidth, from which the attenuation could be inferred, were exhibited recently by Durand and Pine.[8] The experimental techniques developed in this latter work are employed here to obtain the temperature dependence of the sound-wave propagation. Stimulated Brillouin scattering using Q-switched ruby-laser excitation has also been observed in fused quartz.[9–11] In principle, the same information about phonon velocity and damping can be extracted by stimulated methods. Walder and Tang[10] obtained a 300°K damping, in agreement with the data herein when frequency-corrected. However, transient effects may complicate the analysis for the damping.[11]

Closely connected with the theories of acoustic attenuation are the frequencies and densities of states of other thermal-phonon modes and the presence of possible structural relaxations. Such information may be contained in the Raman and infrared spectra of

* This work was sponsored by the Department of the U. S. Air Force.

[1] O. L. Anderson and H. E. Bommel, J. Am. Ceram. Soc. **38**, 125 (1955).

[2] A. S. Pine, in *Light Scattering Spectra of Solids*, edited by G. B. Wright (Springer-Verlag, New York, 1969), p. 581.

[3] C. K. Jones, P. G. Klemens, and J. A. Rayne, Phys. Letters **8**, 31 (1964).

[4] R. S. Krishnan, Proc. Indian Acad. Sci. **A37**, 377 (1953).

[5] P. Flubacher, A. J. Leadbetter, J. A. Morrison, and B. P. Stoicheff, J. Phys. Chem. Solids **12**, 53 (1960).

[6] D. H. Rank and A. E. Douglas, J. Opt. Soc. Am. **38**, 966 (1948).

[7] S. M. Shapiro, R. W. Gammon, and H. Z. Cummins, Appl. Phys. Letters **9**, 157 (1966).

[8] G. Durand and A. S. Pine, IEEE J. Quantum Electron. **4**, 523 (1968).

[9] P. E. Tannenwald, in *Physics of Quantum Electronics*, edited by P. L. Kelley, B. Lax, and P. E. Tannenwald (McGraw-Hill Book Co., New York, 1966), p. 223.

[10] J. Walder and C. L. Tang, Phys. Rev. Letters **19**, 623 (1967).

[11] W. Heinicke and G. Winterling, Appl. Phys. Letters **11**, 231 (1967).

fused quartz. Features of these spectra have indeed been implicated in the previous studies of ultrasonic absorption. We will reexamine these conclusions and present an alternative interpretation which favors our hypothesis of anharmonic acoustic damping.

II. ANHARMONIC AND STRUCTURAL RELAXATION MODELS

We will review briefly two possible mechanisms that could account for the attenuation of sound in fused quartz. The first is an anharmonic or three-phonon interaction, which is the usual cause of such damping if the material exhibits no low-frequency resonances. The second is a structural relaxation process, the existence of which would imply a great deal about the fundamental nature of the glassy state.

The anharmonic model to be considered here was introduced by Bommel and Dransfeld[12] as a qualitative explanation of their acoustic absorption measurements in α-quartz. Their calculation of the damping rate Γ was based on Akhieser's mechanism of sound-induced changes in the thermal-phonon distribution and entropy. For a crystal of density ρ, temperature T, a sound wave of frequency ω and velocity v_l, and a thermal-phonon mode with heat capacity c_v and relaxation time τ, they obtained for the damping

$$\Gamma=\frac{\gamma^2\omega T c_v}{8\rho v_l^2}\frac{\omega\tau}{1+(\omega\tau)^2}. \tag{1}$$

Here γ^2 is an averaged dimensionless Grüneisen constant of order unity which measures the anharmonicity. Γ is related to the acoustic attenuation constant α and the Brillouin linewidth $\delta\nu$ (full width at half-maximum) by

$$\Gamma=\pi\delta\nu=\alpha v_l. \tag{2}$$

Equation (1) is valid under restricted circumstances only.[2] Terms higher than cubic in the anharmonicity have been neglected. Elastic isotropy, both harmonic and anharmonic, have been assumed, and the group velocity of the thermal phonons has been taken to be much smaller than v_l. Only one thermal mode has been considered, and the "dominant-phonon" approximation has been made. The dominant-phonon approximation applies when the frequency and relaxation time of the thermal phonons are not rapid functions of wave vector. In addition, it is required that $kT\gg\hbar\omega$ and that processes involving the decay of the hypersonic wave into lower-frequency phonons are negligible. These latter requirements are well met for typical experimental conditions. Harmonic elastic isotropy is, of course, valid for fused quartz; damping from the scattering of other thermal modes is simply additive.

[12] H. E. Bommel and K. Dransfeld, Phys. Rev. **117**, 1245 (1960).

It is not surprising from the above approximations that Eq. (1) has the form of acoustic damping in liquids due to interaction with molecular internal degrees of freedom.[13] The principal difficulty in applying (1) to the attenuation data is the great uncertainty in the relevant thermal-phonon frequency and lifetime. In general, if Raman and neutron scattering data are not available, these quantities must be estimated from theoretical models.

Woodruff and Ehrenreich[14] derived the acoustic damping for the exceptional case of a Debye spectrum of thermal phonons. These phonons have group velocity v_l and are responsible for the energy or heat transport in a solid. It was then possible to estimate τ from the umklapp relaxation time accessible by thermal conductivity measurements. They obtained a reasonable quantitative fit to Bommel and Dransfeld's data on α-quartz. However, more recent measurements have demonstrated the importance of including dispersion,[15] anisotropy,[16] and distributed normal relaxation processes[2] for the thermal modes.

The simple equation (1), with its restrictions and its relationship to the theories of Woodruff and Ehrenreich and others, is derivable[2] from a more general formulation due to Kwok,[17] and later to Klein.[18] These latter authors extended the Green's-function perturbation method of Maradudin and Fein[19] for the anharmonic interaction problem to considerations of acoustic absorption. The Kwok and Klein theories do not include the effects of temperature- and momentum-shifted thermal-mode distributions which Woodruff and Ehrenreich had discussed for their model. This is equivalent to dropping the vertex contributions in the diagram formalism of Griffin.[20] At present, no complete theory exists from which we could assess the effect of these contributions on Eq. (1).

The thermal-phonon lifetime τ is obtained directly from the basic anharmonic theory of Maradudin and Fein.[19] In general, a vibration of frequency ω_0 is broadened by decay into two other phonons such that $\omega'+\omega''=\omega_0$ and by scattering one mode into another according to $\omega'-\omega''=\omega_0$. The temperature dependence of these processes is primarily contained in the boson factors

$$n'=(e^{\hbar\omega'/kT}-1)^{-1}. \tag{3}$$

For most cases one can simplify the damping contri-

[13] R. Y. Chiao and P. A. Fleury, in *Physics of Quantum Electronics*, edited by P. L. Kelley, B. Lax, and P. E. Tannenwald (McGraw-Hill Book Co., New York, 1966), p. 241.

[14] T. O. Woodruff and H. Ehrenreich, Phys. Rev. **123**, 1553 (1961).

[15] H. J. Maris, Phil. Mag. **9**, 901 (1964).

[16] N. S. Shiren, Phys. Letters **20**, 10 (1966).

[17] P. C. Kwok, Ph.D. thesis, Harvard University, 1965 (unpublished).

[18] R. Klein, Physik Konsierten Materie **6**, 38 (1967).

[19] A. A. Maradudin and A. E. Fein, Phys. Rev. **128**, 2589 (1962).

[20] A. Griffin, Rev. Mod. Phys. **40**, 167 (1968).

butions of the decay and scattering mechanisms to

$$\tau^{-1}=(n'+n''+1)A_0, \tag{4a}$$

$$\tau^{-1}=(n''-n')B_0, \tag{4b}$$

respectively.[21] A_0 and B_0 are complicated integrals involving anharmonic selection rules and joint densities of states at ω' and ω''. In the absence of direct measurement of τ, the factors A_0 and B_0 may be adjusted to fit the data once the thermal-phonon frequencies are chosen. The damping rate Γ of the hypersonic wave is a specialization of the category (4b). There the frequency is so low that ω' and ω'' belong to the same thermal-phonon branch whose lifetime thereby becomes a factor.

We now discuss the structural relaxation mechanism advanced by Anderson and Bommel[1] to explain ultrasonic absorption in fused quartz. The mathematical form of this model is similar to that of the anharmonic model, but the physical mechanism is distinct. Here the damping rate is given by

$$\Gamma=\frac{G\omega(\omega/\Omega)}{1+(\omega/\Omega)^2}. \tag{5}$$

Here Ω is the transition rate or frequency of a structural relaxation, and G is a temperature-independent constant representing the strength of the relaxation.

The particular structural transition postulated by Anderson and Bommel is a reordering of the Si-O-Si bond angle. Such a picture is a convenient visual aid, but let us start with a more general description. We presume that an ion in the disordered structure may reside in a double potential well with a central barrier of activation energy E. The transition rate for jumping between minima is the product of some zero-point vibrational frequency ω_1 in one minimum and the Boltzmann probability of surmounting the barrier. Thus,

$$\Omega=\omega_1 e^{-E/kT}. \tag{6a}$$

Alternatively, if ω_1 is much less than kT/h, then the transition rate is of the Eyring form

$$\Omega=(kT/h)e^{-E/kT}. \tag{6b}$$

Anderson and Bommel hypothesize that an oxygen may be displaced normal to a Si-Si axis if the silicons lie closer together than they do in crystalline quartz. This occurs because the Si-O bond length is nearly the same for the ordered and disordered structures. The double well then arises because the oxygen may have another equilibrium position on the opposite side of the Si-Si axis, assuming rotations about the axis are inhibited. The data of Anderson and Bommel could be fitted arbitrarily well with a distribution of relaxation terms of type (6b). Such a distribution could be expected for the random silica lattice where several different bond angles may occur, each with its own activation energy and relaxation strength.

[21] A. S. Pine and P. E. Tannenwald, Phys. Rev. (to be published).

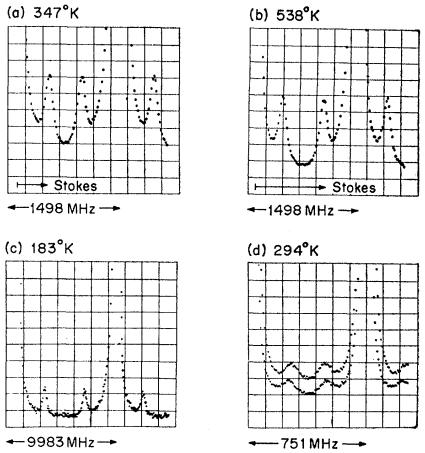

FIG. 1. Brillouin spectra of longitudinal hypersonic waves in fused quartz. The temperatures and free spectral range of the interferometers are indicated. All traces are Suprasil except the upper (d), which is Corning high-optical-quality fused quartz.

The mathematical similarity between the anharmonic and structural relaxation models is apparent from Eqs. (1) and (5). It is also possible to identify τ^{-1} of (4b) with Ω of (6b). At very low temperatures such that $kT/\hbar\ll\omega''$ or ω_0, $\tau^{-1}\sim e^{-\hbar\omega''/kT}$; at high temperatures such that $kT/\hbar\gg\omega'$, $\tau^{-1}\sim T$. Thus, the two models have the same asymptotic temperature behavior if we identify $\hbar\omega'$ with the activation energy.

III. EXPERIMENTAL RESULTS

Although the attenuation of hypersound in fused quartz is extremely high by the standards of pulse-echo techniques, the damping is generally lower than one encounters in liquids.[13] At room temperature and above, the high-resolution system described by Durand and Pine[8] is used to record the Brillouin spectrum. A single-mode He-Ne laser of 150 μW is the source; the back-scattered light is analyzed in a piezoelectric multi-scanned confocal spherical interferometer; a low-dark-count photomultiplier feeding a synchronously swept multichannel analyzer registers the spectrum. Typical Brillouin spectra of fused quartz at various temperatures are shown in Fig. 1. Note that the intense Rayleigh peak triggers the analyzer so that slow drift of the spectrometer is automatically compensated in the accumulated spectrum. Such stabilization is necessary because of the long integration times required to enhance the signal-to-noise ratio of the extremely weak scattered light. Below room temperature, where the sound absorption increases and the total scattering decreases proportionally to T, the above system over-resolves the natural linewidth and yields a critically weak spectrum. For this reason, a lower-resolution pressure-scanned plane-parallel interferometer is used

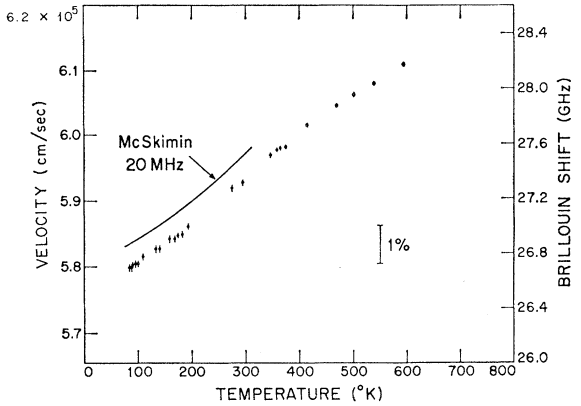

FIG. 2. Velocity and Brillouin shift of longitudinal acoustic phonons in fused quartz.

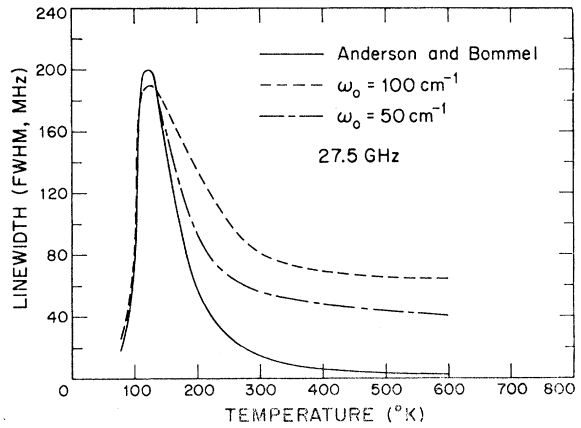

FIG. 4. Theoretical models of hypersonic damping in fused quartz.

with concomitant lesser stability and shorter integration times, resulting in larger inaccuracies in the data. Though this system could also be multiply scanned, fluctuations in the room temperature and pressure limited the reproducibility of the slow sweep rate.

The fused-quartz sample is a 2.5-cm-diam cylinder of Suprasil, 5 cm long, with optically polished ends. Temperature is measured with a thermocouple in contact with the sample's circumference less than 1 cm from the scattering volume. Thermal environment is provided by an evacuated Dewar or oven with a single window to minimize spurious light reflected in the backward direction.

The experimental velocity of sound and Brillouin shift are plotted as a function of temperature in Fig. 2. These data are compared with the ultrasonic measurements of McSkimin[22] at 20 MHz in a material supplied by Amersil. Though it is tempting to ascribe the decrease in velocity of the hypersonic data from the ultrasonic to dispersion, it is possible that sample dependence or inaccuracy of the ultrasonic time-of-flight absolute measurement are responsible for the discrepancy. Calibration of the Brillouin shift using several interferometer spacers is better than 0.2%. The relative precision of the thermal variation of the shift is about 0.02%. As seen in Fig. 1(d), a sample of Corning high-optical-quality fused quartz is found to have a velocity 0.04% higher than Suprasil at room temperature.

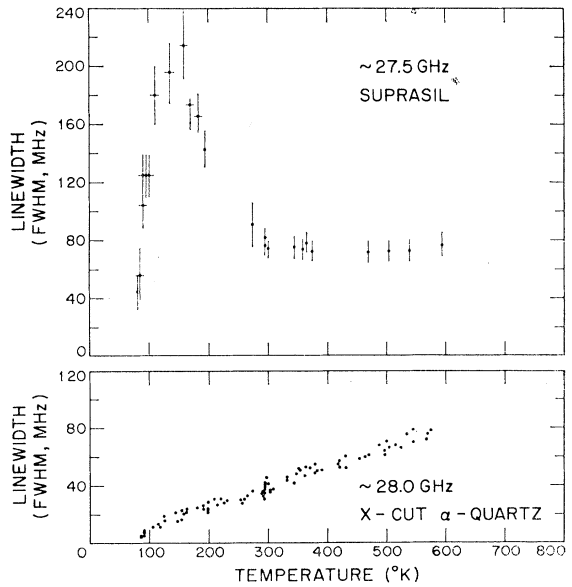

FIG. 3. Damping of longitudinal hypersonic waves: (a) fused quartz; (b) α-quartz along the X axis.

[22] H. J. McSkimin, J. Appl. Phys. 24, 988 (1953).

Brillouin linewidth data for fused quartz are plotted in Fig. 3(a). The data reduction procedure by which the natural linewidths are deconvolved from the experimental spectra is described at some length in the Appendix. For purposes of comparison, linewidth data for α-quartz are presented in Fig. 3(b). These results and their possible interpretation have been reported in more detail previously.[2] The broad low-temperature peak in the absorption of fused quartz is clearly a distinct and challenging feature. This peak has been the focus of interest in many previous ultrasonic experiments.[1,3,23] Lack of resolution and scattering intensity prevent an extension of the measurements to lower temperatures where Jones *et al.*[3] observed subsidiary peaks. Higher-temperature data could not be reliably obtained because of severe thermal gradients in the sample caused by radiation. These gradients yield an artificial broadening over the scattering volume, since the velocity is a function of temperature. Obviously, it would be interesting to see if the fused-quartz absorption ever drops below the "intrinsic" level in crystalline quartz at higher temperatures.

IV. DISCUSSION

We now compare the anharmonic and structural relaxation models with the available acoustic absorption data in fused quartz. The temperature dependence

[23] M. E. Fine, H. Van Duyne, and N. T. Kenney, J. Appl. Phys. 25, 402 (1954).

of the absorption and the frequency dependence of the temperature and damping at the peak are the interesting features to be explained. In Fig. 4 we apply the theory of Anderson and Bommel[1] to the hypersound damping. Two possible anharmonic channels are superimposed for comparison. Each of the models has been normalized for a rough fit to the Brillouin scattering data.

The parameters used for the two anharmonic processes are (a) $\omega_0=100$ cm^{-1}, $\omega'=500$ cm^{-1}, $\omega''=400$ cm^{-1}, $B_0=3\times10^{13}$ sec^{-1}, and $A_0=0$, and (b) $\omega_0=50$ cm^{-1}, $\omega'=450$ cm^{-1}, $\omega''=400$ cm^{-1}, $B_0=10^{14}$ sec^{-1}, and $A_0=0$. Thus decay of the thermal phonon at ω_0 has been neglected. Bommel and Anderson chose their parameter $E=1030$ cal/mole$\simeq$375 cm^{-1} and placed an arbitrary factor of 0.8 in Eq. (6b) to improve their fit. There is one less adjustable parameter per mode in the structural relaxation theory but there is much poorer agreement with the data. As previously mentioned, this situation may be remedied by including a distribution of structural transitions and thereby increasing the number of parameters. Of course, this is also true of the anharmonic models but fewer modes appear to be necessary. At lower acoustic frequencies, both models predict too narrow a temperature width to the damping peak.

The peak absorption occurs at a temperature such that $\omega\tau=1$ or $\omega=\Omega$. Because of the mathematical similarity between Ω and τ^{-1}, there is little difference in the two theoretical predictions of the frequency dependence of the peak temperature. In Fig. 5 this similarity is illustrated. The data are accumulated in Table I from the work of Fine *et al.*,[23] Anderson and Bommel,[1] Jones *et al.*,[3] and this paper. Although the anharmonic model appears to fit the data better, the older model could be improved by slightly readjusting the parameters in light of the more recent data.

A more crucial test arises from the behavior of the magnitude of the peak absorption versus frequency. From the experimental sources above, the peak loss factor increases slowly with frequency as seen in Fig. 6. The loss factor is variously defined as the internal friction (Q^{-1}), the attenuation per wavelength ($\alpha\lambda/\pi$), or the linewidth divided by the frequency ($\delta\nu/\nu$).

TABLE I. Ultrasonic data in fused quartz at the absorption peak.

Acoustic frequency (MHz)	Peak temperature (°K)	Peak loss	Ref.
0.050	36	$Q^{-1}=11.5\times10^{-4}$	23
0.126	37	$Q^{-1}=11.5\times10^{-4}$	23
0.066	35	$Q^{-1}=8.3\times10^{-4}$	1
0.201	39	$Q^{-1}=9.4\times10^{-4}$	1
20	46	$Q^{-1}=18.8\times10^{-4}$	1
330	60	$\alpha=36$ dB/cm	3
507		$\alpha=62$ dB/cm	3
748		$\alpha=83$ dB/cm	3
930	67	$\alpha=113$ dB/cm	3
26 820	130	$\delta\nu=200$ MHz	This work

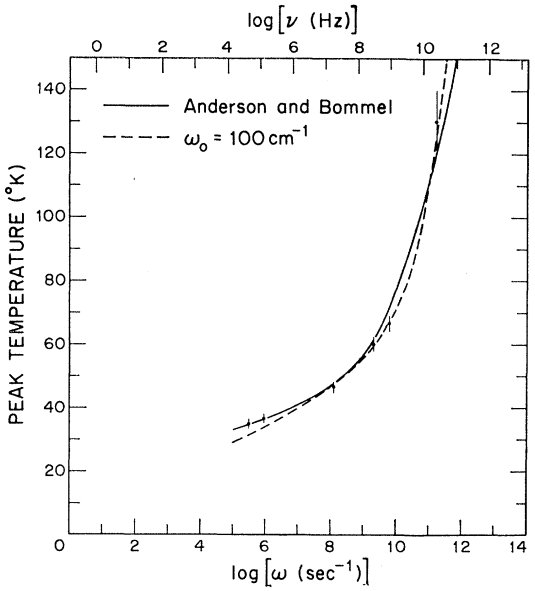

FIG. 5. Frequency dependence of temperature at acoustic absorption peak in fused quartz. (The base of the logarithms is 10.)

From Eq. (5) it is obvious that a single structural relaxation results in a peak loss factor equal to G which is independent of frequency. Aware of this failure, Anderson and Bommel demonstrated that a distribution of relaxation terms could account for the experimental results, at least at low frequencies. On the other hand, a single anharmonic process does produce an increasing loss factor with frequency. This occurs through the TC_v term in Eq. (1), since the peak temperature is a function of frequency as we have just discussed. We have plotted the single-channel theories in Fig. 6 using an Einstein-type specific heat for the thermal phonons at $\omega_0=50$ and 100 cm^{-1}.

In order to select the most likely acoustic damping mechanism it is useful to examine other physical evidence and consequences of the two models. Anderson and Bommel cite as possible evidence of their structural

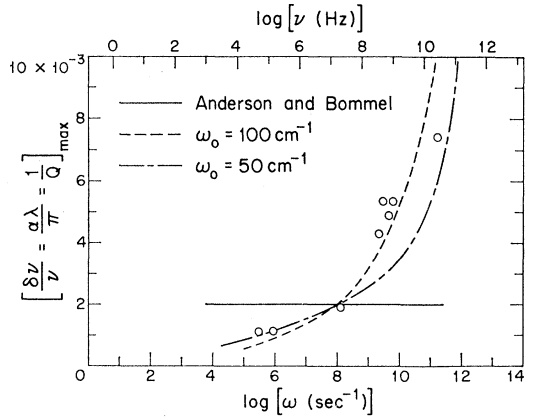

FIG. 6. Frequency dependence of peak loss factor in fused quartz. (The base of the logarithms is 10.)

transitions a strongly depolarized Raman band at ~ 30 cm^{-1} seen by Rank and Douglas.[6] This is the room-temperature frequency Ω calculated to fit the acoustic absorption. However, this prominent low-frequency band is only observed in a lead glass and not in a silicate-rich material[6]; nor has such structure been reported in fused quartz and certainly no feature with the temperature dependence of Ω has been seen.

The existence of low-frequency modes, perhaps of structural transition origin, is implied by two other phenomena in fused quartz. The first is the rf dielectric loss[24] which has roughly the same frequency-temperature behavior as the acoustic loss. Assuming these to have a common cause, the structural transition model predicts that the rf couples directly to the ion oscillating in the double well. The rf loss can also be explained by the anharmonic model as a second-order scattering process analogous to the two-phonon difference bands in infrared absorption.

The second evidence for low-lying modes is the anomalous low-temperature heat capacity of fused quartz. Flubacher *et al.*[5] attribute the anomaly to the presence of three low-frequency modes which they select from their continuum Raman spectrum. Though they note the Anderson-Bommel structural relaxation, they suggest that the relevant motion is a translation or libration of a molecular grouping such as an SiO_4 tetrahedron. There is, however, a serious question as to the interpretation of the Raman or infrared low-frequency continuum as a manifestation of low-lying optical modes. Stolen[25] has remarked that a heat capacity calculation using the *actual* Raman distribution of modes does not agree with measurements nearly as well as the three modes arbitrarily selected by Flubacher *et al.* Further, Dawber and Elliott[26] have shown that the ir spectrum of a disordered crystal contains a component which reflects the perfect-crystal density of states. The same is true of the Raman spectrum,[27] so the continuum of fused quartz may essentially arise from the acoustic and lower optical phonon branches in crystalline quartz.

The same view of the Raman spectrum, as the disorder-induced one-phonon density of states, provides a firmer basis for the anharmonic model. The thermal-phonon frequencies ω_0, ω', and ω'' used to fit the data are all close to identifiable features of the spectrum of Flubacher *et al.* The α-quartz progenitors of the two ω_0 channels would probably be the 128-cm^{-1} E mode and the lowest zone-edge TA branch near 50 cm^{-1}. The fused-quartz ir transmission measurements of Plendl *et al.*[28] also show structure near 120 cm^{-1}. Since the spectral distribution of these modes is inhomogeneous, their natural lifetime is masked. We must then look elsewhere for an estimate of τ which would confirm our choice of parameters in the anharmonic model.

Pine and Tannenwald[21] studied the temperature dependence of the lifetime of the 128-cm^{-1} vibration in α-quartz. Because this mode is the lowest-lying optical phonon, it can only decay into a relatively small density of acoustic phonon states. Therefore, at low temperatures, where scattering processes are frozen out, the residual damping of this mode is much smaller than for any other Raman line in α-quartz. However, this residual width is still considerably larger than the damping of the analogous 100-cm^{-1} mode in fused quartz required to explain the hypersonic absorption. On the other hand, the lowest zone-edge acoustic branch cannot decay because of energy and momentum conservation conditions. These phonons are bottlenecked, as Orbach and Vredevoe[29] describe, and only scattering processes are available to damp them.

Since we had to neglect decay processes in order to have τ fit the hypersonic attenuation data, it appears that the most likely candidate for the thermal mode ω_0 is the lowest zone-edge acoustic branch at 50 cm^{-1}. Although this mode does not fit the experiment as well as the 100-cm^{-1} mode, as seen from Figs. 4 and 3(a), this may simply be a limitation of the single relaxation theory. Probably a component of the "intrinsic" absorption of Fig. 3(b) is operative in the fused-quartz results. Of course, the intrinsic absorption is basically the same anharmonic mechanism involving the *upper* acoustic branch.[2] An unanswered question is: Why are only the phonons around 400–500 cm^{-1} effectively scattered by the mode at ω_0? These are the major peaks in the fused-quartz Raman spectrum, but scattering of lower modes is indicated in α-quartz.[21]

In summary, it is seen that the acoustic and dielectric losses are not uniquely explained by a structural relaxation mechanism. On balance the anharmonic model appears to fit the hypersonic attenuation data with fewer parameters. These parameters may be reasonably justified in terms of recently measured lattice spectra of quartz and more modern interpretations. The Anderson-Bommel parameters are based on a more speculative model of the dynamical structure of fused quartz. Of course, many aspects of the anharmonic model are untested and any definite conclusion must await a detailed temperature study of the Raman and neutron spectra of fused quartz.

ACKNOWLEDGMENTS

The author is grateful to Dr. R. Stolen of Bell Telephone Laboratories for discussing some of his

[24] J. M. Stevels, discussed in Ref. 1.

[25] R. Stolen (private communication); for interpretation of the ir spectrum see W. Bagdade and R. Stolen, J. Phys. Chem. Solids **29**, 2001 (1968).

[26] P. G. Dawber and R. J. Elliott, Proc. Roy. Soc. (London) **273**, 222 (1963); Proc. Phys. Soc. (London) **81**, 453 (1963).

[27] N. D. Strahm, Ph.D. thesis MIT, 1969 (unpublished). The work of D. W. Feldman, J. H. Parker, W. J. Choyke, and L. Patrick [Phys. Rev. **173**, 787 (1968)] is relevant by extension to random polymorphs.

[28] J. N. Plendl, L. C. Mansur, A. Hadni, F. Brehat, P. Henry, G. Morlot, F. Naudin, and P. Strimer, J. Phys. Chem. Solids **28**, 1589 (1967).

[29] R. Orbach and L. A. Vredevoe, Physics **1**, 91 (1964).

Raman data and specific heat calculations prior to publication. Also he is indebted to Dr. P. E. Tannenwald for his very helpful comments on the manuscript.

APPENDIX

The deconvolution procedure used to analyze the data is illustrated here by example. The procedure is similar to that used by others[30,31] to extract spectral line shapes from instrumentally broadened contours. In Fig. 7 we show the instrumental profile $I(\nu)$, the experimental data $E(\nu)$, the observed Brillouin peaks $E'(\nu)=E(\nu)-I(\nu)$, with the background and overlap visually subtracted out, and the deconvolved Lorentzian spectral distribution $L(\nu)$. The raw data are the same as those in Fig. 1(a).

The instrumental profile for the confocal Fabry-Perot (free spectral range 1498 MHz, finesse 40) is entered digitally into a computer for a numerical convolution integration. The computer is programmed to generate Lorentzian functions $L_i(\nu)=[1+(2\nu/\delta\nu_i)^2]^{-1}$ for various full widths $\delta\nu_i$. These Lorentzians are convolved with $I(\nu)$ until the resultant spectrum has the same full width at half-maximum (FWHM) as the observed contour $E'(\nu)$. The FWHM of the matching Lorentzian $\delta\nu_L$ is printed out together with the point-by-point convolved spectrum $I(\nu)\otimes L(\nu)$. The latter may be compared with $E'(\nu)$ as in Fig. 7 to demonstrate that the Lorentzian spectral distribution properly represents the true line shape. A small angular broadening $\delta\nu_\theta$ due to the finite collection solid angle is then subtracted from $\delta\nu_L$ to give the natural width $\delta\nu_{\mathrm{FWHM}}$ presented in Fig. 3(a). This angular broadening in fused quartz is simply induced by the angular dependence of the Brillouin shift,[8] so

$$\delta\nu_\theta\simeq-\nu(\delta\theta)^2/8\simeq 5\ \mathrm{MHz}, \qquad (7)$$

where $\delta\theta$ is a measure of the half-angle of collection inside the sample. In principle, this spectral shift should be incorporated in the theoretical distribution before convolution with $I(\nu)$, but the correction is small and does not noticeably affect the fit of the convolved line shape with $E'(\nu)$.

The accuracy of this procedure is as good as the linewidth measurement of $E'(\nu)$. Of course, this varies for the data at different temperatures because of the varying signal-to-noise ratios and varying interferometer resolution. The signal-to-noise ratio of the multiscan data [e.g., Fig. 1(a) and 1(b)] is about 10 times that of the pressure-scan data [e.g., Fig. 1(c)], since the integration times for the former are 100 sec and for the latter 2 sec. Furthermore, linewidth data are given only when the observed width exceeds the instrumental resolution by at least 50% for the pressure-scanned Fabry-Perot data and 100% for the multiscanned. The results are spot-checked against spectra taken with the very-high-resolution interferometer shown in Fig. 1(d). The convolution errors are reduced greatly when the natural width is many times that of the instrument, but of course the signal-to-noise ratio is reduced since the spectrum is overresolved. To reduce the errors from overlap of the Brillouin components with each other or with the laser line, no linewidth data have been entered where the Brillouin peak falls outside the range 0.22–0.40 interorders.

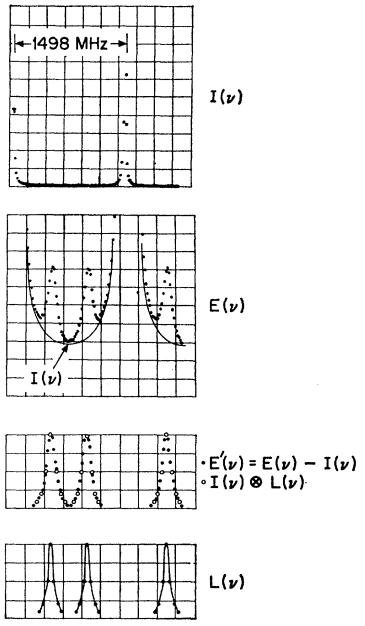

FIG. 7. Sample deconvolution of Brillouin scattering data. $I(\nu)$, instrumental profile $E(\nu)$, experimental data, $E'(\nu)$, observed Brillouin spectrum with background subtracted off, $L(\nu)$, Lorentzian convolved with $I(\nu)$ to match $E'(\nu)$; $L(\nu)$ hand-sketched from computer-generated $\delta\nu_L=82$ MHz.

It is of interest to point out that the Fabry-Perot profile $I(\nu)$ closely approximates the theoretical Airy function

$$I(\nu)\simeq[1+(2\Delta\nu/\pi\delta\nu_I)^2\sin^2(\pi\nu/\Delta\nu)]^{-1}, \qquad (8)$$

where $\Delta\nu$ is the free spectral range and $\delta\nu_I$ is the instrumental full width. For large finesse, this function resembles a Lorentzian with slightly compressed wings. If $I(\nu)$ were exactly Lorentzian, the convolved spectrum would be a Lorentzian whose width would be the sum of $\delta\nu_I$ and $\delta\nu_L$. In reality, as with the Airy function, the convolved spectrum is a near-Lorentzian with compressed wings and with a width less than the sum of $\delta\nu_I$ and $\delta\nu_L$. Experimentally, we have observed that the Lorentzian width $\delta\nu_L$ is always about 10% higher than the width obtained by straightforward subtraction.

[30] T. J. Greytak and G. B. Benedek, Phys. Rev. Letters **17**, 179 (1966); T. J. Greytak, Ph.D. thesis, MIT, 1967 (unpublished).
[31] W. R. L. Clements and B. P. Stoicheff, Appl. Phys. Letters **12**, 246 (1968).